

# Hydrogen/nitrogen/oxygen defect complexes in silicon from computational searches

Andrew J. Morris <sup>\*,1</sup> Chris J. Pickard,<sup>2</sup> and R. J. Needs<sup>1</sup>

<sup>1</sup>*Theory of Condensed Matter Group, Cavendish Laboratory, University of Cambridge,  
J. J. Thomson Avenue, Cambridge CB3 0HE, United Kingdom*

<sup>2</sup>*Department of Physics and Astronomy, University College London, Gower St, London WC1E 6BT, United Kingdom*  
(Dated: October 31, 2018)

Point defect complexes in crystalline silicon composed of hydrogen, nitrogen, and oxygen atoms are studied within density-functional theory (DFT). *Ab initio* Random Structure Searching (AIRSS) is used to find low-energy defect structures. We find new lowest-energy structures for several defects: the triple-oxygen defect,  $\{3O_i\}$ , triple oxygen with a nitrogen atom,  $\{N_i, 3O_i\}$ , triple nitrogen with an oxygen atom,  $\{3N_i, O_i\}$ , double hydrogen and an oxygen atom,  $\{2H_i, O_i\}$ , double hydrogen and oxygen atoms,  $\{2H_i, 2O_i\}$  and four hydrogen/nitrogen/oxygen complexes,  $\{H_i, N_i, O_i\}$ ,  $\{2H_i, N_i, O_i\}$ ,  $\{H_i, 2N_i, O_i\}$ , and  $\{H_i, N_i, 2O_i\}$ . We find that some defects form analogous structures when an oxygen atom is replaced by a NH group, for example,  $\{H_i, N_i, 2O_i\}$  and  $\{3O_i\}$ , and  $\{H_i, N_i\}$  and  $\{O_i\}$ . We compare defect formation energies obtained using different oxygen chemical potentials and investigate the relative abundances of the defects.

PACS numbers: 61.05.-a, 61.72.jj

## I. INTRODUCTION

Hydrogen (H) is a common impurity in silicon (Si) which is particularly important as a passivator of surfaces and bulk defects.<sup>1</sup> The role of hydrogen in semiconductors is highlighted in a review by Estreicher.<sup>2</sup> Adding nitrogen (N) impurities to silicon affects the formation of voids and may increase the strength of the silicon crystal by immobilising dislocations, which reduces warping during wafer processing.<sup>3</sup> The majority of silicon used in device technologies is manufactured in a quartz crucible by the Czochralski (Cz) process, during which oxygen (O) from the quartz readily enters the melt, see for example the review by Newman.<sup>4</sup>

A wide variety of experimental probes are used to study defects in silicon, but it is often difficult to determine their detailed structures from measurements alone. Theoretical studies using *ab initio* techniques are helpful in this regard, as they are used to calculate both the defect formation energies and some of their experimental signatures. For example, local vibrational modes of defects are accessible to infra-red (IR) absorption experiments and may also be calculated within *ab initio* methods.

Throughout this paper we denote a defect complex by listing its constituent atoms between braces,  $\{A_i, B_s, \dots\}$ , where a subscript denotes whether an atom is substitutional (s) or interstitial (i). For example, a defect containing two interstitial hydrogen atoms and a substitutional nitrogen atom is denoted by  $\{2H_i, N_s\}$ . Despite hydrogen and nitrogen being common impurities in silicon, we are aware of only one *ab initio* theoretical study of their interaction.<sup>5</sup> It was concluded that both  $\{N_s\}$  and  $\{N_i\}$  defects are able to trap hydrogen atoms, although with smaller binding energies than that of a hydrogen atom and a vacancy. The Fourier transform infra-red (FTIR) vibrational line at  $2967\text{cm}^{-1}$  found in silicon prepared in a hydrogen atmosphere is assigned to the N–H stretch mode of

the  $\{H_i, N_i\}$  defect.<sup>6</sup> Interstitial oxygen may be present in Cz-Si in concentrations as high as  $10^{18}\text{cm}^{-3}$ . Oxygen impurity atoms may be used for gettering metallic impurities, which increases the overall crystal quality, but they also form electrically active thermal donors (TD).<sup>7</sup> TDs can affect the local resistivity within the silicon wafer.<sup>8</sup> In addition, oxygen also interacts with nitrogen in bulk silicon to form TDs, and small concentrations of hydrogen can greatly enhance the formation of TDs.<sup>9</sup> It has been shown that the presence of hydrogen molecules in silicon crystals enhances the diffusion of oxygen. It has also been suggested that hydrogen passivates the electrical activity of N/O complexes in Cz-Si.<sup>10</sup>

It is clear from these examples that the interactions between hydrogen, nitrogen, and oxygen impurities in silicon lead to important and complicated behavior. Here we present the results of a computational search for low-energy defect complexes in silicon containing hydrogen, nitrogen, and oxygen atoms. We confirm the stability of many of the previously-known defects and also report the structures and formation energies of some new low-energy defects. To the best of our knowledge, this is the first time that all of these defects have been compared within a single study.

The rest of this paper is set out as follows, in Sec. II we discuss the computational methods used in the study. In Sec. III we describe the calculation of the defect formation energies and explain our choice of chemical potentials. Results for H/N defects are presented in Sec. IV, N/O defects in Sec. V, H/O defects in Sec. VI, and H/N/O defects in Sec. VII. The relative abundances of the defects are studied in Sec. VIII and a discussion of our results is presented in Sec. IX.

## II. COMPUTATIONAL APPROACH

### A. Random Structure Searching

“*Ab initio* random structure searching” (AIRSS) has already proved to be a powerful tool for finding crystalline structures of solids under high pressures.<sup>11,12,13,14,15,16</sup> The

\*Email: ajm255@cam.ac.uk.

basic algorithm is very simple: we take a population of random structures and relax them to local minima in the energy. Pickard and Needs<sup>11</sup> showed that “random structure searching” can be applied to finding structures of point defects, and the approach is discussed in more detail in Ref. 17.

Creating the initial simulation cell is a three-stage process. First, we choose the size of the disruption to the perfect silicon lattice by defining the radius of a sphere in which the impurity atoms are to be placed randomly. We choose radii between 3 and 7 Å. Secondly, we chose the number of silicon atoms to have their positions randomized. In this study we randomize the position of 1 to 3 silicon atoms depending on the number of hydrogen, nitrogen and oxygen impurity atoms present. The randomization sphere is centered on the centroid of the removed silicon atoms. Finally, the required number of hydrogen, nitrogen and oxygen impurity atoms and the chosen 1, 2 or 3 silicon atoms are placed at random positions within the sphere. The configurations are then relaxed using the calculated density-functional-theory (DFT) forces.

### B. Density-functional-theory calculations

Our calculations are performed using the Generalized Gradient Approximation (GGA) density functional of Perdew, Burke, and Ernzerhof (PBE).<sup>18</sup> We use the plane-wave basis-set code CASTEP,<sup>19</sup> with its built-in ultrasoft pseudopotentials<sup>20</sup> which include non-linear core corrections.<sup>21</sup> All of the results presented here are for non-spin-polarized systems. The multi-Baldereschi k-point scheme described in Ref. 17 is used for sampling the Brillouin zone. We perform the same computational convergence tests as described in Ref. 17, finding excellent convergence with a  $2 \times 2 \times 2$  k-point sampling, which we use for all the results reported here.

The searches we report in this paper are carried out in a body-centered-cubic simulation cell which would hold 32 atoms of crystalline silicon. Although this is a small cell, tests indicate that it is adequate for obtaining good structures for most of the defects studied and reasonably accurate formation energies, while keeping the computational cost low enough to permit extensive searching. In a previous study,<sup>17</sup> we reported results for hydrogen/silicon complexes in silicon. The searches were carried out in the same 32-atom cell used here, but each of the defect structures was re-relaxed in a 128-atom cell to obtain more accurate structures and energies. The defect formation energies for the 32-atom cells were not reported, but they are in fact in excellent agreement with the 128-atom values. Consider, for example, the calculations for an interstitial silicon atom (denoted by  $I$ ) and hydrogen impurity atoms in crystalline silicon reported in Ref. 17. The changes in the formation energies on increasing the cell size from 32 to 128 atoms for the defects  $\{I, H\}$ ,  $\{I, H_2\}$ ,  $\{I, H_3\}$  and  $\{I, H_4\}$  are only 0.00,  $-0.07$ ,  $-0.01$  and  $-0.02$  eV, respectively. We have also compared our results for N/O defects in silicon with data from the literature. Fujita *et al.*<sup>22</sup> used DFT and 216-atom cells to calculate the binding energies for the following defect reactions in silicon:  $\{2N_i, O_i\} + \{O_i\} \rightarrow$

$\{2N_i, 2O_i\}$ ,  $\{2N_i\} + \{O_i\} \rightarrow \{2N_i, O_i\}$ , and  $\{N_i, O_i\} + \{O_i\} \rightarrow \{N_i, 2O_i\}$ , obtaining 0.91, 0.98, and 1.12 eV, respectively, in good agreement with our 32-atom cell results of 0.80, 0.91 and 0.97 eV, respectively. Finally, Coutinho *et al.*<sup>23</sup> used DFT and 64-atom cells to calculate the formation energy of the  $\{O_i\}$  defect, obtaining values between 1.989 and 1.820 eV, depending on the basis set used, which is in good agreement with our value of 1.90 eV. We should not, of course, expect a 32-atom cell to be sufficient for all point-defect calculations in silicon, and especially not for charged defect states, but there is a strong case for believing it to be adequate for the purposes of the current study.

### III. CALCULATING THE FORMATION ENERGIES

In order to define defect formation energies it is necessary to specify the chemical potentials of the atomic species. The chemical potential for silicon is taken to be the bulk silicon value, so that the energy cost to add a silicon atom to a defect is the energy of a silicon atom in perfect crystalline silicon. The chemical potential for hydrogen is derived from the lowest energy hydrogen defect in silicon, which is an interstitial molecule at the tetrahedral site,  $\{H_2 i\}$ , with the bond pointing along a  $\langle 100 \rangle$  direction. This is the same chemical potential as used in our study of hydrogen impurities in silicon.<sup>17</sup> We use the most energetically favorable nitrogen defect,  $\{2N_i\}$ ,<sup>5,24,25,26,27</sup> to set the chemical potential of nitrogen.

We perform around 130 AIRSS searches with one, two, three, or four interstitial oxygen atoms per cell. The lowest energy  $\{O_i\}$  defect found is the buckled-bond-centered configuration which has been studied extensively.<sup>23,28,29,30,31,32</sup> The  $\{2O_i\}$  defect has two buckled-bond-centered oxygen atoms bonded to a silicon atom. This defect was reported in Ref. 23 and is known as the staggered  $\{2O_i\}$  defect.

Our searches also find the previously-reported staggered chain  $\{3O_i\}$  defect.<sup>30,33,34,35,36,37</sup> We find a new structure, see Fig. 1, with a formation energy 0.15 eV lower than the staggered chain. To the best of our knowledge this defect has not been mentioned before. We also find the  $\{4O_i\}$  defect which was previously reported as the  $O_4(1,1)$  defect in Ref. 38.

Table I shows the formation energies per oxygen atom of the four oxygen defects and quartz, using the chemical potential of the  $\{O_i\}$  defect as the reference for supplying oxygen atoms. We note that the formation energy decreases with each additional oxygen, showing that oxygen defects tend to aggregate, the lowest possible energy being achieved by forming crystalline  $\text{SiO}_2$  (quartz).

We consider three different chemical potentials for oxygen. These correspond to choosing the source of oxygen atoms as  $\mu_{\{O_i\}}$ ,  $\mu_{\{4O_i\}}$ , and  $\mu_{\text{quartz}}$ . The chemical potential  $\mu_{\{nO_i\}}$  for oxygen with the source of oxygen atoms being the  $\{nO_i\}$  defect is calculated as the energy of the lowest-energy structure of the 32-atom silicon cell containing  $n$  oxygen atoms and the energy of the 32-atom bulk silicon cell, divided by  $n$ . The  $\{O_i\}$  defect gives the highest oxygen chemical potential, while quartz gives the lowest chemical potential. We include

the chemical potential,  $\mu_{\text{quartz}}$ , calculated from quartz, since it is the opposite extreme to  $\mu_{\{\text{O}_i\}}$  in terms of oxygen saturation.

Defect	$E_f$ per O (eV)
O	0.00
2O	-0.25
3O	-0.42
4O	-0.46
Quartz	-1.90

TABLE I: Formation energies per oxygen atom for different oxygen complexes, relative to the oxygen bond-centered defect ( $\text{O}_{\text{bc}}$ ). These values can also be thought of as the oxygen chemical potentials relative to a source of oxygen atoms consisting of single-oxygen defects.

Defect	$\text{O}_i$	$4\text{O}_i$	Quartz	Saturation
Bulk	0.00	0.00	0.00	✓
$\{2\text{N}_i\}$	0.00	0.00	0.00	✓
$\{\text{O}_i\}$	0.00	0.46	1.90	✓
$\{2\text{O}_i\}$	-0.50	0.42	3.29	✓
<b><math>\{3\text{O}_i\}</math></b>	-1.27	0.12	4.41	✓
$\{4\text{O}_i\}$	-1.85	0.00	5.73	✓
$\{\text{H}_2\}_i$	0.00	0.00	0.00	✓
$\{\text{H}_i, \text{N}_i\}$	0.45	0.45	0.45	✓
$\{\text{H}_i, \text{N}_s\}$	0.81	0.81	0.81	✓
<b><math>\{2\text{H}_i, \text{N}_s\}</math></b>	0.76	0.76	0.76	×
$\{\text{N}_i, \text{O}_i\}$	0.43	0.89	2.32	×
$\{\text{N}_i, 2\text{O}_i\}$	-0.54	0.39	3.25	×
$\{\text{N}_i, 3\text{O}_i\}$	-0.92	0.49	4.76	×
$\{2\text{N}_i, 2\text{O}_i\}$	-1.71	-0.78	2.09	✓
$\{2\text{N}_i, \text{O}_i\}$	-0.91	-0.44	0.99	✓
<b><math>\{3\text{N}_i, \text{O}_i\}</math></b>	0.15	0.61	2.05	×
$\{\text{H}_i, \text{O}_i\}$	0.65	1.11	2.54	×
$\{\text{H}_i, 2\text{O}_i\}$	-0.04	0.89	3.75	×
<b><math>\{2\text{H}_i, \text{O}_i\}</math></b>	-0.23	0.23	1.67	✓
<b><math>\{2\text{H}_i, 2\text{O}_i\}</math></b>	-0.76	0.17	3.03	✓
<b><math>\{\text{H}_i, \text{N}_i, \text{O}_i\}</math></b>	-0.68	-0.22	1.21	✓
<b><math>\{2\text{H}_i, \text{N}_i, \text{O}_i\}</math></b>	-0.26	0.20	1.63	×
<b><math>\{\text{H}_i, 2\text{N}_i, \text{O}_i\}</math></b>	-0.49	-0.03	1.40	×
<b><math>\{\text{H}_i, \text{N}_i, 2\text{O}_i\}</math></b>	-0.85	0.08	2.94	✓

TABLE II: Formation energies defined by Eq. (1) in eV for various H/N/O complexes with three different choices of the oxygen chemical potential. The final column indicates whether the system could form a structure with fully-saturated covalent bonding (✓), or whether it cannot (×), see Sec. IX. The defect structures shown in bold have not, to the best of our knowledge, been reported in the literature before.

The formation energy of a defect,  $E_f$ , is defined as

$$E_f = E_D - \sum_i n_i \mu_i, \quad (1)$$

where  $n_i$  is the number of each atomic type  $i$  in the defect cell of energy  $E_D$ , and the chemical potentials,  $\mu_i$ , are defined above.

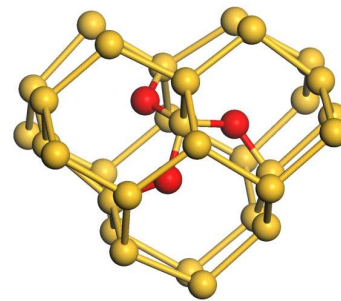


FIG. 1: (Color online) The  $\{3\text{O}_i\}$  defect is composed of three buckled-bond-centered oxygen atoms, each bonded to a single, four-fold coordinated silicon atom. Silicon atoms are shown in yellow and oxygen atoms in red.

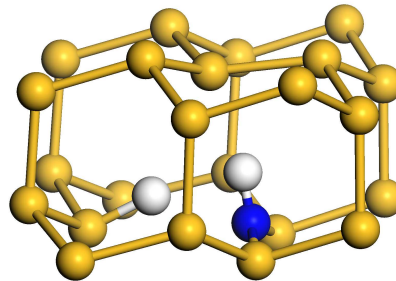


FIG. 2: (Color online) The first metastable H/N defect,  $\{2\text{H}_i, \text{N}_s\}$ , contains a three-fold coordinated nitrogen atom close to a lattice site. One of the hydrogen atoms is bonded directly to the nitrogen atom and points toward a neighboring three-fold coordinated silicon atom. The remaining hydrogen atom terminates a dangling bond on another neighboring silicon atom. The silicon atoms are shown in yellow, the nitrogen in blue and the hydrogen atoms in white.

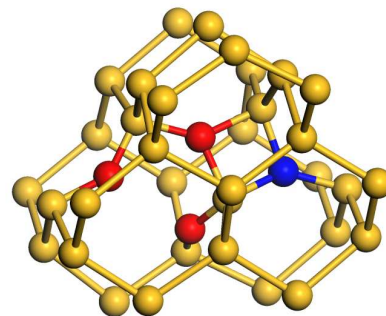


FIG. 3: (Color online) The  $\{\text{N}_i, 3\text{O}_i\}$  defect contains a four-atom ring consisting of a nitrogen atom, an oxygen atom and two silicon atoms. The two other oxygen atoms are in buckled-bond-centered positions. Note that the structure contains an over-coordinated oxygen atom with three bonds. The silicon atoms are shown in yellow, the nitrogen in blue, and the oxygen atoms in red.

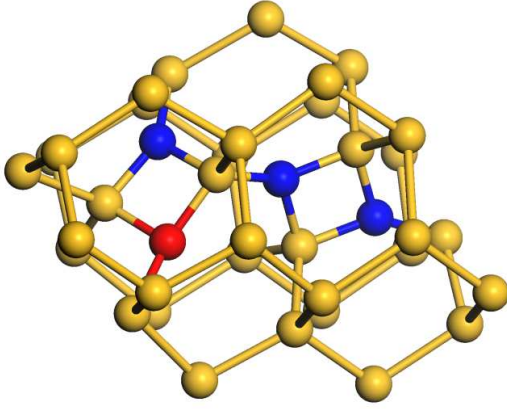


FIG. 4: (Color online) The lowest-energy  $\{3N_i, O_i\}$  defect consists of a four-atom ring of two nitrogen atoms and two silicon atoms adjacent to another four-atom ring of an oxygen atom, a nitrogen atom and two silicon atoms. Note that the structure contains an over-coordinated oxygen atoms with three bonds. The silicon atoms are in yellow, the nitrogen atoms in blue and the oxygen atom in red.

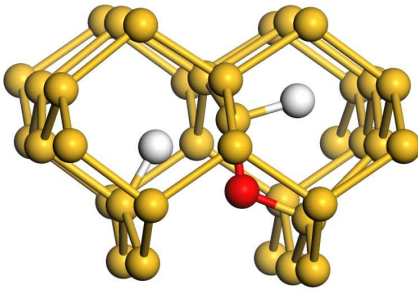


FIG. 5: (Color online) The  $\{2H_i, O_i\}$  defect is composed of a buckled-bond-centered oxygen atom adjacent to a distorted  $\{H_2\}^*$  defect. The silicon atoms are shown in yellow, the oxygen atom in red and the hydrogen atoms in white. This defect has a negative formation energy, showing that the metastable  $\{H_2\}^*$  defect<sup>39</sup> is stabilized by the presence of oxygen.

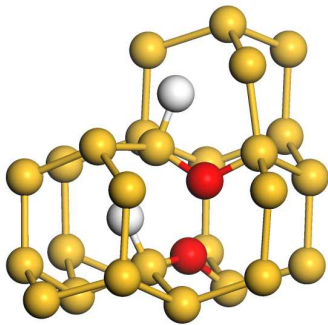


FIG. 6: (Color online) The  $\{2H_i, 2O_i\}$  defect is composed of two adjacent  $\{H_i, O_i\}$  defects. The silicon atoms are shown in yellow, the oxygen atom in red and the hydrogen atoms in white.

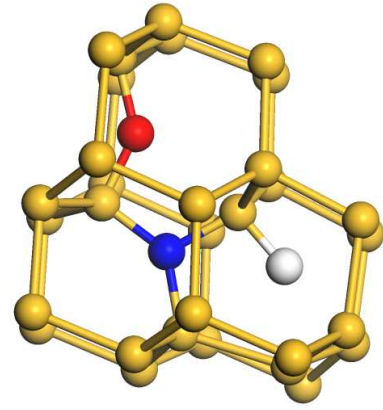


FIG. 7: (Color online) The  $\{H_i, N_i, O_i\}$  defect contains a nitrogen and silicon atom sharing a lattice site, with the dangling silicon bond terminated by the hydrogen atom. A nearest-neighbor silicon atom of the nitrogen atom is bonded to a buckled-bond-centered oxygen atom. The silicon atoms are shown in yellow, the oxygen in red, the nitrogen in blue and the hydrogen in white.

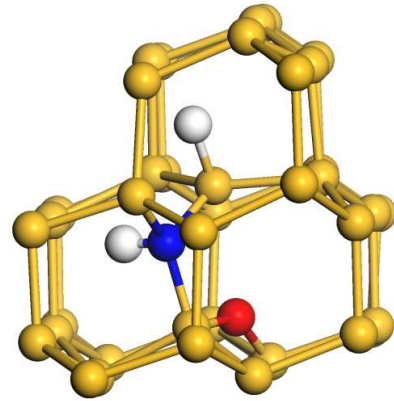


FIG. 8: (Color online) The  $\{2H_i, N_i, O_i\}$  defect is similar to the  $\{H_i, N_i, O_i\}$  defect but with the nitrogen atom acquiring the extra hydrogen atom, making it over-coordinated with four bonds. This defect has the highest formation energy of all the H/N/O defects studied and is therefore unlikely to form. The silicon atoms are shown in yellow, the oxygen in red, the nitrogen in blue and the hydrogen atoms in white.

#### IV. H/N DEFECTS

We have relaxed around 250 different starting structures for the H/N defects using cells containing 32 silicon atoms, 1 nitrogen atom and 1 hydrogen atom, and further searches with 31 silicon atoms, 1 nitrogen atom and 1 hydrogen atom, and with 31 silicon atoms, 1 nitrogen atom and 2 hydrogen atoms. These are the only calculations reported in this paper where we change the number of silicon atoms in the cell. We find defects which we may describe as bulk silicon with an interstitial nitrogen atom and an interstitial hydrogen atom,  $\{H_i, N_i\}$ , bulk silicon with a substitutional nitrogen atom and an inter-

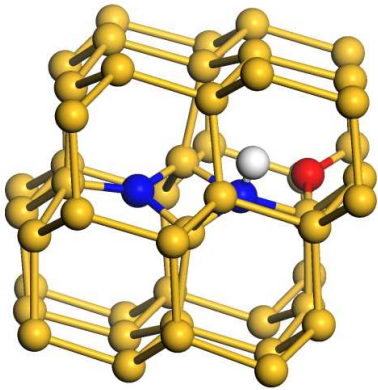


FIG. 9: (Color online) The  $\{H_i, 2N_i, O_i\}$  defect contains a four-atom ring of two nitrogen atoms and two silicon atoms. One of the nitrogen atoms is over-coordinated and is bonded to the hydrogen atom. A nearest-neighbor silicon atom to this nitrogen atom is also bonded to a buckled-bond-centered oxygen atom. The silicon atoms are shown in yellow, the oxygen in red, the nitrogen in blue and the hydrogen in white.

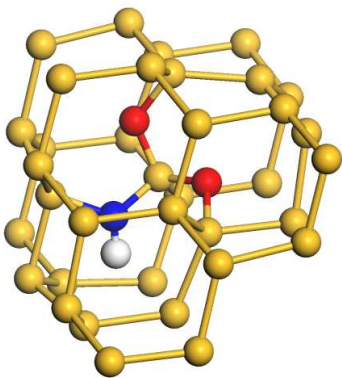


FIG. 10: (Color online) The  $\{H_i, N_i, 2O_i\}$  defect is very similar to the  $\{3O_i\}$  defect, but with one of the oxygen atoms replaced by a NH group. The silicon atoms are shown in yellow, the oxygen in red, the nitrogen in blue and the hydrogen in white.

stitial hydrogen atom,  $\{H_i, N_s\}$ , and bulk silicon with a substitutional nitrogen atom and two interstitial hydrogen atoms,  $\{2H_i, N_s\}$ .

The most stable H/N structure we find is the  $\{H_i, N_i\}$  defect with  $C_s$  symmetry. In this defect the hydrogen atom is bonded to the buckled-bond-centered nitrogen atom, which is three-fold coordinated, the nitrogen, hydrogen, and two silicon atoms lie in a plane. The N–Si bond lengths are both about 1.71 Å and the N–H bond-length is 1.03 Å, in good agreement with McAfee *et al.*,<sup>5</sup> who found bond lengths of 1.73 Å and 1.05 Å, respectively.

The first metastable defect we find,  $\{2H_i, N_s\}$ , is shown in Fig. 2 and has  $C_{3v}$  symmetry. This is quite a complicated defect, and it is energetically slightly more favorable than the

$\{H_i, N_s\}$  defect which is described below.  $\{2H_i, N_s\}$  looks similar to the  $\{H_i, N_s\}$  defect but with the extra hydrogen atom bonded to the three-fold coordinated nitrogen atom.

Finally, we report the  $\{H_i, N_s\}$  defect. This is similar to the  $C_{3v}$  symmetry  $\{N_s\}$  defect,<sup>5</sup> but with the hydrogen atom bonded to the three-fold coordinated silicon atom, increasing its coordination number to four. The three N–Si bonds are all 1.85 Å long, the same as in  $\{N_s\}$ . The N–H distance is 1.95 Å and the H–Si bond is 1.80 Å long, in good agreement with McAfee *et al.*<sup>5</sup>

All of the H/N complexes we mention in this section have  $E_f > 0$ , and hence they are unlikely to form spontaneously.

## V. N/O DEFECTS

Our searches for the N/O complexes required around 1800 random starting structures. These searches found all the previously-known lowest-energy structures except the  $\{2N_i, 2O_i\}$  defect. The  $\{2N_i, 2O_i\}$  defect is quite large and it is probable that we have not relaxed a sufficiently large number of starting structures to find it.

For the  $\{N_i, O_i\}$  defect we obtain the previously-known interstitial ring.<sup>40</sup> This defect has a positive  $E_f(O_i)$  of 0.43 eV, and hence is unlikely to form. The structure of our  $\{N_i, 2O_i\}$  defect is the same as found in previous studies.<sup>22,40,41</sup> This defect has a negative  $E_f(O_i)$  of  $-0.54$  eV, and therefore it could form in silicon.

We are not aware of any previous reports of the  $\{N_i, 3O_i\}$  defect, which is shown in Fig. 3. The  $\{N_i, 3O_i\}$  defect has a negative  $E_f(O_i)$  of  $-0.92$  eV, showing that a single bond-centered oxygen atom will bind to the  $\{N_i, 2O_i\}$  defect.

Our searches for the  $\{2N_i, 2O_i\}$  defect did not yield the structure reported previously,<sup>42</sup> which has different oxygen positions. We generated the structure reported by Fujita *et al.*<sup>42</sup> “by hand” and found it to be 0.19 eV lower in energy than our best structure. The defect of Fujita *et al.*<sup>42</sup> has a negative formation energy of  $E_f(O_i) = -1.71$  eV, and the formation energy remains negative even when the reference structure for the oxygen chemical potential is taken to be that of the  $\{4O_i\}$  defect in silicon. It is disappointing that our searches has not given the previously-known lowest-energy  $\{2N_i, 2O_i\}$  defect. However, we have included the lowest-energy known structure in our analysis of the relative populations of the various defects presented in Sec. VIII.

We find the previously-known lowest-energy  $\{2N_i, O_i\}$  defect,<sup>40,41,42,43</sup> which has a formation energy of  $E_f(O_i) = -0.91$  eV. This defect binds oxygen very strongly and  $E_f(O_i)$  remains negative even with the oxygen chemical potential from the  $\{4O_i\}$  defect.

We are not aware of any previous reports of the  $\{3N_i, O_i\}$  defect in the literature, which is shown in Fig. 4. The  $\{3N_i, O_i\}$  defect is quite large and it may not be well described within a 32-atom cell.

## VI. H/O DEFECTS

We have relaxed around 350 starting structures for the H/O defects. The lowest energy  $\{H_i, O_i\}$  defect that we find is composed of a buckled-bond-centered oxygen atom adjacent to a buckled-bond-centered hydrogen atom. This structure was also found by Estreicher.<sup>44,45</sup> This defect has, however, been the subject of some controversy, as Jones *et al.*<sup>46,47</sup> proposed that the hydrogen atom is attached to a silicon atom at an anti-bonding site. Our search also finds this defect configuration, but we calculate it to be 0.32 eV higher in energy than the ground state structure.

Our lowest-energy  $\{H_i, O_i\}$  defect has a positive formation energy, and hence it is unlikely to form. The  $\{2H_i, 2O_i\}$  defect is composed of two such defects in close proximity to one another, as shown in Fig. 6. The defect has a negative formation energy and, to our knowledge, it has not been presented in the literature previously.

The lowest-energy  $\{2H_i, O_i\}$  defect that we find (Fig. 5) adopts a  $\{H_2\}^*+O_{bc}$  configuration. Measurements have shown an IR absorption line at  $1075.1 \text{ cm}^{-1}$  which has been assigned to a  $O_i-H_2$  complex.<sup>48</sup> However, the  $\{H_2\}^*+O_{bc}$  configuration of the  $\{2H_i, O_i\}$  defect does not contain a hydrogen molecule, see Fig. 5. We also find a  $\{2H_i, O_i\}$  defect structure containing a hydrogen molecule, but it is metastable with an energy 0.26 eV above our ground-state structure. To the best of our knowledge the  $\{H_2\}^*+O_{bc}$  defect structure has not been reported previously.

Our most stable  $\{H_i, 2O_i\}$  defect is a  $O_{bc}+O_{bc}+H$  configuration. This defect has also been studied by Rashkeev *et al.* (see Fig. 3(a) of Ref. 36), who report it to be a thermal double donor (TDD).

The  $\{H_i, 2O_i\}$ ,  $\{2H_i, O_i\}$  and  $\{2H_i, 2O_i\}$  defects all have negative formation energies  $E_f(O_i)$  and are therefore likely to form in bulk silicon.

## VII. H/N/O DEFECTS

We have performed around 500 structural relaxations for the H/N/O defects. The four defects  $\{H_i, N_i, O_i\}$  (Fig. 7),  $\{2H_i, N_i, O_i\}$  (Fig. 8),  $\{H_i, 2N_i, O_i\}$  (Fig. 9), and  $\{H_i, N_i, 2O_i\}$  (Fig. 10), all have negative formation energies when using  $E_f(O_i)$ , and  $\{H_i, N_i, O_i\}$  and  $\{H_i, 2N_i, O_i\}$  also have negative formation energies when using  $E_f(4O_i)$ .

The  $\{H_i, N_i, O_i\}$  defect has a formation energy of  $-0.68 \text{ eV}$  compared with  $0.43 \text{ eV}$  for  $\{N_i, O_i\}$ . This implies that hydrogen readily binds to the  $\{N_i, O_i\}$  defect. The hydrogen atom bonds to a silicon atom and breaks the third bond of the over-coordinated oxygen atom, giving the structure shown in Fig. 7. This results in a defect with fully saturated bonds which is therefore quite low in energy.

The  $\{2H_i, N_i, O_i\}$  defect is very similar to the  $\{H_i, N_i, O_i\}$  defect mentioned above. The extra hydrogen atom bonds to the nitrogen atom which is then over-coordinated, having four bonds, see Fig. 8. The over-coordinated nitrogen atom is energetically unfavorable and this defect would not readily form

from  $\{H_i, N_i, O_i\}$ , however it could form from  $\{N_i, O_i\}$  by capturing a hydrogen molecule.

The  $\{H_i, 2N_i, O_i\}$  defect is an interesting case. The nitrogen atom is over-coordinated because it binds to the hydrogen atom, see Fig. 9. Since  $\{2N_i, O_i\}$  has a formation energy of  $-0.91 \text{ eV}$  and  $\{H_i, 2N_i, O_i\}$  has a formation energy of  $-0.49 \text{ eV}$  it is unlikely that a hydrogen atom will bind to  $\{2N_i, O_i\}$ .

The  $\{H_i, N_i, 2O_i\}$  defect is very interesting. The fully-saturated bonding of this defect results in a low formation energy of  $-0.85 \text{ eV}$ . This is lower than the formation energy of  $\{N_i, 2O_i\}$ , and hydrogen will therefore bind to this defect. The  $\{H_i, N_i, 2O_i\}$  defect has a similar geometry to  $\{3O_i\}$ , but with one of the oxygen atoms replaced by a HN group. A HN group acting in a similar fashion to an oxygen atom was also observed in the  $\{N_i, H_i\}$  defect of McAfee,<sup>5</sup> which looks similar to the bond-centered  $\{O_i\}$  defect.

## VIII. RELATIVE ABUNDANCES

The formation energies of the various defects can be used to calculate the relative abundances of the defects at zero temperature as a function of the ratios of the H/N/O concentrations. The relative abundances for a chosen set of concentrations are those which minimise the total energy, and the chemical potentials do not enter the calculation. However, if we allow the oxygen atoms to combine with silicon to form quartz, it is straightforward to show that the minimum energy is always obtained by producing as much quartz as possible, so that no point defects containing oxygen atoms remain in the bulk, and the hydrogen and nitrogen atoms form  $\{H_2\}$  and  $\{2N_i\}$  defects. This is inconsistent with the extensive experimental evidence for other point defects in silicon involving hydrogen, nitrogen, and oxygen atoms. To gain some insight into the H/N/O defects which may be present we must therefore limit the propensity to form quartz and other low-energy oxygen defects in some way. We have chosen to present relative abundances in which the formation of  $\{2O_i\}$ ,  $\{3O_i\}$ ,  $\{4O_i\}$ , up to quartz are excluded, while allowing the formation of  $\{O_i\}$ . This is an arbitrary choice, but it serves to illustrate the type of behavior which may arise. Figs. 11, 12, and 13 show relative abundances of the defects as a function of the H/N/O concentrations. In each figure we keep the concentrations of two of the species constant and equal to unity, while the concentration of the third impurity varies from zero to three. The main features of Figs. 11, 12, and 13 are that, for equal concentrations of hydrogen, nitrogen, and oxygen, the dominant defects are hydrogen molecules and the  $\{2N_i, 2O_i\}$  defect. Varying the nitrogen or oxygen concentration leads to the formation of a wide variety of defects. Increasing the hydrogen concentration, however, only generates more hydrogen molecules. Other scenarios can be investigated using the data given in Table II.

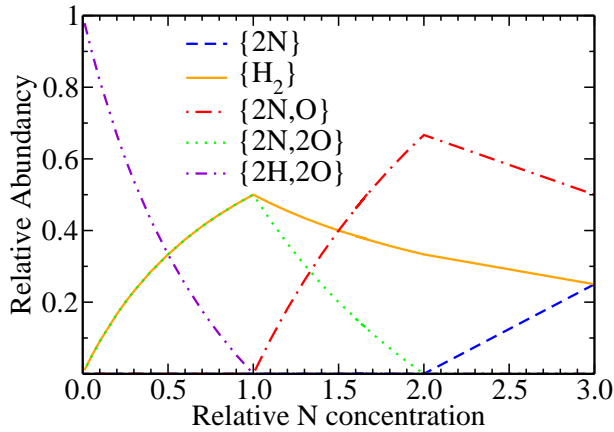


FIG. 11: (Color online) Relative concentrations of H/N/O defects in silicon as a function of the nitrogen concentration. At low nitrogen concentrations ( $H:N:O = 1:<0.5:1$ ), the predominant defect is  $\{2H_i, 2O_i\}$ . As the nitrogen concentration increases the concentration of  $\{2H_i, 2O_i\}$  decreases, with  $\{2N_i, 2O_i\}$  and molecular hydrogen being formed. As the nitrogen concentration increases above unity, the concentration of  $\{2N_i, 2O_i\}$  declines and  $\{2N_i, O_i\}$  begins to form. At nitrogen concentrations larger than two, the additional nitrogen atoms form  $\{2N_i\}$  defects.

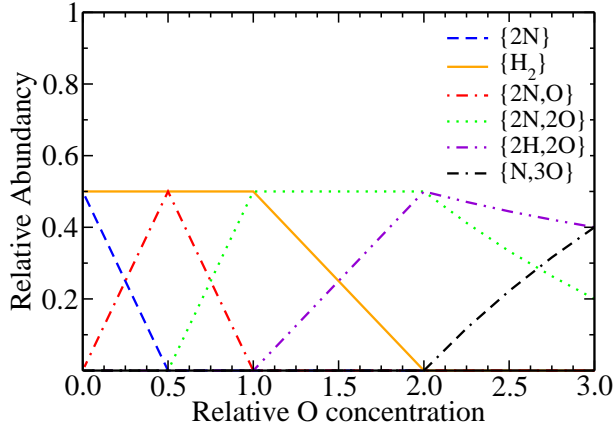


FIG. 12: (Color online) Relative concentrations of H/N/O defects in silicon as a function of the oxygen concentration. The behavior is complex in this case, although the general trend is simply that the more stable defects containing larger numbers of oxygen atoms are favored at higher oxygen concentrations.

## IX. DISCUSSION

We have presented *ab initio* calculations of H/N/O complexes in bulk silicon within DFT. The defect complexes were generated in 32-atom supercells using the AIRSS method as outlined in Ref. 17. The 32-atom cells are large enough to give a reasonable description of most of the defects, but small enough to allow extensive searching. To the best of our knowledge this is the first time that H/N/O complexes in silicon have been studied in detail.

AIRSS searches were performed on oxygen, hydrogen, and nitrogen defects to evaluate chemical potentials for the atoms.

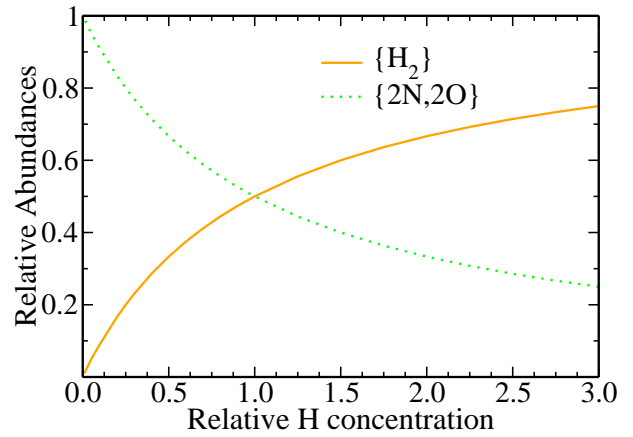


FIG. 13: (Color online) Relative concentrations of H/N/O defects in silicon as a function of the hydrogen concentration. Increasing the hydrogen concentration simply generates more interstitial hydrogen molecules.

Whilst carrying out the searches on oxygen defects, we discovered a new  $\{3O_i\}$  defect, shown in Fig. 1, which is more stable than the staggered defect which has been reported in the literature.

Our searches reproduced all of the previously-known lowest-energy H/N complexes. We have also described a new metastable  $\{2H_i, N_s\}$  defect which is more favorable than some of the other H/N complexes presented in the literature.

The searches for N/O complexes were slightly less successful. We were unable to find the previously-known  $\{2N_i, 2O_i\}$  defect. In this case, we performed DFT calculations on the previously-known best structure for comparison. We discovered a new  $\{3N_i, O_i\}$  defect (Fig. 4) and a new  $\{N_i, 3O_i\}$  defect (Fig. 3) which is more stable than the  $\{N_i, 2O_i\}$  defect, implying that an oxygen atom could bind to  $\{N_i, 2O_i\}$ .

Our searches reproduced all of the previously-known lowest-energy H/O complexes. We find the  $\{H_i, O_i\}$  defect to have a positive formation energy, and therefore it is unlikely to form, but two adjacent  $\{H_i, O_i\}$  defects can form a  $\{2H_i, 2O_i\}$  defect (Fig. 6) which has a formation energy of  $E_f(O_i) = -0.76$  eV. We also find a new  $\{2H_i, O_i\}$  defect which is based on the previously-reported metastable  $H_2^*$  defect.<sup>39</sup> The  $\{2H_i, O_i\}$  defect has  $E_f(O_i) = -0.23$  eV, showing that the  $H_2^*$  defect can bind an oxygen atom.

To the best of our knowledge, no previous discussion of H/N/O complexes in silicon has appeared in the literature. The  $\{H_i, N_i, O_i\}$  and  $\{H_i, N_i, 2O_i\}$  defects are more energetically favorable than their non-hydrogen-containing counterparts  $\{N_i, O_i\}$ ,  $\{N_i, 2O_i\}$ , showing that many of these defects could exist in hydrogenated forms.

Another point of interest is that H/N complexes behave in an analogous fashion to oxygen defects. For example, the  $\{H_i, N_i\}$  defect adopts a buckled-bond-centered arrangement with the hydrogen atom terminating the dangling bond on the nitrogen atom. The nitrogen atom takes a similar position to the oxygen atom in the  $O_{bc}$  defect, however without the hydrogen atom, since oxygen forms only two covalent bonds. The same relationship holds between the  $\{3O_i\}$  and  $\{H_i, N_i, 2O_i\}$

defects, where again the H/N group in the latter behaves like an  $O_{bc}$  defect in the former.

The right-hand column of Table II indicates whether or not it is possible for the indicated set of atoms to form a fully-saturated covalently-bonded structure. In such a structure each silicon atom is bonded to four other atoms, each nitrogen to three, each oxygen to two, and each hydrogen to one. As each bond is shared between two atoms, a fully-saturated covalently-bonded structure is impossible if

$$4N_{Si} + 3N_N + 2N_O + N_H = \text{odd number}, \quad (2)$$

where  $N_X$  denotes the number of atoms of type X in the cell. We note from the data in Table II that the lowest energy defects are normally those having completely saturated bonds. A similar result for hydrogen defects in silicon was reported in Ref. 17. This simple and rather obvious rule is useful for choosing combinations of impurity atoms which might form stable defects.

Consider a host crystal containing three types of impurity atom. (An example might be H/N/O impurities in silicon as studied here, but without the possibility of silicon vacancy formation which was allowed in our study of H/N defects.) Limiting the total number of impurity atoms to be  $\leq 4$  gives 34 possible cell contents for which searches must be performed. Increasing the number of possible impurities to five (while maintaining the maximum number of impurities in a cell to be  $\leq 4$ ) gives a total of 125 possible cell contents. The extra impurities could be other types of atoms, but they could also be

host vacancies  $V$  and interstitials  $I$ , although this would reduce the number of possible cell contents to 112 because introducing a host vacancy and interstitial is the same as not introducing either. Searching over the ‘‘impurities’’ H/N/O/I/V in silicon, with a maximum number of impurities of  $\leq 4$  and the same computational parameters as in the present study would cost about three times as much as the present study. For each set of cell contents we have in this work performed between about 20–900 structural relaxations, which appeared to be adequate in this case, although the required number is expected to increase rapidly with the size of the ‘‘hole’’ in the host crystal. In some cases it may be necessary to use larger ‘‘holes’’ to obtain all of the low-energy defects, and perhaps larger simulation cells as well. We have automated the search procedure and the calculations are performed in parallel. It appears to us that defect structure searches of the type described in this paper with up to, say, five types of impurity are perfectly feasible with modern computing facilities.

### Acknowledgments

We are grateful to Phil Hasnip and Michael Rutter for useful discussions. This work was supported by the Engineering and Physical Sciences Research Council (EPSRC) of the United Kingdom. Computational resources were provided by the Cambridge High Performance Computing Service.

- 
- <sup>1</sup> C. G. Van de Walle and J. Neugebauer, *Annu. Rev. Mater. Res.* **36**, 179 (2006).
  - <sup>2</sup> S. K. Estreicher, *Mater. Sci. Eng.* **R 14**, 319 (1995).
  - <sup>3</sup> K. Sumino, I. Yonenaga, M. Imai, and T. Abe, *J. App. Phys.* **54**, 5016 (1983).
  - <sup>4</sup> R. C. Newman, *J. Phys: Condens. Matter* **12**, R335 (2000).
  - <sup>5</sup> J. L. McAfee, H. Ren, and S. K. Estreicher, *Phys. Rev. B* **69**, 165206 (2004).
  - <sup>6</sup> B. Pajot, B. Clerjaud, and Z.-J. Xu, *Phys. Rev. B* **59**, 7500 (1999).
  - <sup>7</sup> Proceedings of the GADEST Conferences [Solid State Phenom. **108-109**, 97-123 (2005)], [*ibid.* **95-96**, 539-586].
  - <sup>8</sup> J. Härkönen, E. Tuovinen, P. Luukka, E. Tuominen, Z. Li, A. Ivanov, E. Verbitskaya, V. Eremin, A. Pirojenko, I. Riikimäki and A. Virtanen, *Nucl. Instr. and Meth.* **541**, 202 (2005).
  - <sup>9</sup> H. J. Stein and S. Hahn, *J. App. Phys.* **75**, 3477 (1994).
  - <sup>10</sup> X. Pi, D. Yang, X. Ma, Q. Shui, and D. Que, *Phys. Stat. Sol. B* **221**, 641 (2000).
  - <sup>11</sup> C. J. Pickard and R. J. Needs, *Phys. Rev. Lett.* **97**, 045504 (2006).
  - <sup>12</sup> C. J. Pickard and R. J. Needs, *Nature Physics* **3**, 473 (2007).
  - <sup>13</sup> C. J. Pickard and R. J. Needs, *Phys. Rev. B* **76**, 144114 (2007).
  - <sup>14</sup> C. J. Pickard and R. J. Needs, *Nature Materials* (2008).
  - <sup>15</sup> C. J. Pickard and R. J. Needs, *Phys. Rev. Lett.* **102**, 125702 (2009).
  - <sup>16</sup> C. J. Pickard and R. J. Needs, *Phys. Rev. Lett.* **102**, 146401 (2009).
  - <sup>17</sup> A. J. Morris, C. J. Pickard, and R. J. Needs, *Phys. Rev. B* **78**, 184102 (2008).
  - <sup>18</sup> J. P. Perdew, K. Burke, and M. Ernzerhof, *Phys. Rev. Lett.* **77**, 3865 (1996).
  - <sup>19</sup> S. J. Clark, M. D. Segall, C. J. Pickard, P. J. Hasnip, M. I. J. Probert, K. Refson and M. C. Payne, *Z. Kristallogr* **220**, 567 (2005).
  - <sup>20</sup> D. Vanderbilt, *Phys. Rev. B* **41**, 7892 (1990).
  - <sup>21</sup> S. G. Louie, S. Froyen, and M. L. Cohen, *Phys. Rev. B* **26**, 1738 (1982).
  - <sup>22</sup> N. Fujita, R. Jones, S. Öberg, and P. R. Briddon, *App. Phys. Lett.* **91**, 051914 (2007).
  - <sup>23</sup> J. Coutinho, R. Jones, P. R. Briddon, and S. Öberg, *Phys. Rev. B* **62**, 10824 (2000).
  - <sup>24</sup> R. Jones, S. Öberg, F. Berg Rasmussen, and B. Bech Nielsen, *Phys. Rev. Lett.* **72**, 1882 (1994).
  - <sup>25</sup> N. Fujita, R. Jones, J. P. Goss, P. R. Briddon, T. Frauenheim and S. Öberg, *App. Phys. Lett.* **87**, 021902 (2005).
  - <sup>26</sup> J. P. Goss, I. Hahn, R. Jones, P. R. Briddon, and S. Öberg, *Phys. Rev. B* **67**, 045206 (2003).
  - <sup>27</sup> H. Sawada and K. Kawakami, *Phys. Rev. B* **62**, 1851 (2000).
  - <sup>28</sup> S. Hao, L. Kantorovich, and G. Davies, *Phys. Rev. B* **69**, 155204 (2004).
  - <sup>29</sup> H. Yamada-Kaneta, C. Kaneta, and T. Ogawa, *Phys. Rev. B* **42**, 9650 (1990).
  - <sup>30</sup> M. Pesola, J. von Boehm, T. Mattila, and R. M. Nieminen, *Phys. Rev. B* **60**, 11449 (1999).
  - <sup>31</sup> E. Artacho *et al.*, *Phys. Rev. B* **56**, 3820 (1997).
  - <sup>32</sup> J. Plans, G. Diaz, E. Martinez, and F. Yndurain, *Phys. Rev. B* **35**, 788 (1987).
  - <sup>33</sup> L. Tsetseris, S. Wang, and S. T. Pantelides, *App. Phys. Lett.* **88**,



- 051916 (2006).
- <sup>34</sup> Y. J. Lee, M. Pesola, J. von Boehm, and R. M. Nieminen, *Phys. Rev. B* **66**, 075219 (2002).
- <sup>35</sup> M. Pesola, Y. Joo Lee, J. von Boehm, M. Kaukonen, and R. M. Nieminen, *Phys. Rev. Lett.* **84**, 5343 (2000).
- <sup>36</sup> S. N. Rashkeev, M. D. Ventra, and S. T. Pantelides, *App. Phys. Lett.* **78**, 1571 (2001).
- <sup>37</sup> D. J. Chadi, *Phys. Rev. Lett.* **77**, 861 (1996).
- <sup>38</sup> Y. J. Lee and R. M. Nieminen, *Comp. Phys. Comm.* **142**, 305 (2001).
- <sup>39</sup> K. J. Chang and D. J. Chadi, *Phys. Rev. B* **40**, 11644 (1989).
- <sup>40</sup> H. Ono, *App. Phys. Express* **1**, 025001 (2008).
- <sup>41</sup> A. Gali, J. Miro, P. Deák, C. P. Ewels, and R. Jones, *J. Phys: Condens. Matter* **8**, 7711 (1996).
- <sup>42</sup> N. Fujita, R. Jones, S. Oberg, and P. R. Briddon, *J. Mater. Sci. Mater. Electron* **18**, 683 (2007).
- <sup>43</sup> R. Jones, C. Ewels, J. Goss, J. Miao, P. Deák, S. Oberg and F. Berg Rasmussen, *Semicond. Sci. Technol.* **9**, 2145 (1994).
- <sup>44</sup> S. K. Estreicher, *Phys. Rev. B* **41**, 9886 (1990).
- <sup>45</sup> M. Ramamoorthy and S. T. Pantelides, *Solid State Commun.* **106**, 243 (1998).
- <sup>46</sup> R. Jones, S. Öberg, and A. Umerski, *Mater. Sci. Forum* **83**, 551 (1992).
- <sup>47</sup> R. Jones, W. Jackson, A. M. Stoneham, R. C. Newman, and M. Symons, *Phil. Trans. Roy. Soc. Lon. Ser. A* **350**, 1693 (1995).
- <sup>48</sup> V. P. Markevich and M. Suezawa, *J. Appl. Phys.* **83**, 2988 (1998).